Articles

Structure of the Dinuclear Active Site of Urease. X-ray Absorption Spectroscopic Study of Native and 2-Mercaptoethanol-Inhibited Bacterial and Plant Enzymes

Shengke Wang,[†] Mann H. Lee,[‡] Robert P. Hausinger,[*,‡] Patrick A. Clark,[§] Dean E. Wilcox,[*,§] and Robert A. Scott[*,†]

Departments of Chemistry and Biochemistry and Center for Metalloenzyme Studies, University of Georgia, Athens, Georgia 30602-2556, Departments of Microbiology and Biochemistry, Michigan State University, East Lansing, Michigan 48824-1101, and Department of Chemistry, Dartmouth College, Hanover, New Hampshire 03755

Received February 26, 1993[⊗]

The structures of the dinuclear Ni(II) active sites of urease from jack bean and *Klebsiella aerogenes* are compared with and without the addition of the inhibitor 2-mercaptoethanol (2-ME). No significant differences are observed by nickel K-edge X-ray absorption spectroscopy between the plant and bacterial enzymes. The Ni X-ray absorption edge spectra display an 8332-eV 1s → 3d peak intensity similar to that observed for five-coordinate Ni(II) compounds[1] for both native and 2-ME-bound derivatives. Curve-fitting of Ni EXAFS data indicates that the average Ni(II) coordination environment in native urease can be described as Ni(imidazole)$_x$(N,O)$_{5-x}$, with x = 2 or 3. Addition of 2-ME results in replacement of one of the non-imidazole (N,O) ligands with (S,Cl) (most likely the thiolate sulfur of 2-ME) and results in the appearance of a new peak in the Fourier transforms that can only be fit with a Ni···Ni scattering component at a Ni–Ni distance of ~3.26 Å. A structure for this 2-ME-bound dinuclear site is proposed to contain the two Ni(II) ions bridged by the thiolate sulfur of 2-ME.

Introduction

Urease (EC 3.5.1.5) is a Ni-dependent enzyme that catalyzes the hydrolysis of urea to form ammonia and carbonic acid.[2,3] The enzyme is present in a variety of plants, selected fungi, and a broad range of bacterial species, but the most detailed biochemical analyses have involved proteins isolated from *Canavalia ensiformis* (jack bean) and *Klebsiella aerogenes*. Though differing greatly in subunit composition, the homohexameric plant enzyme (subunit M_r 90 770[4]) and the heteropolymeric (M_r 11 086, 11 695, and 60 309[5]) bacterial enzyme exhibit over 50% identity in sequences and each possesses two nickel ions per catalytic unit.[6,7] As described below, the nickel in urease has been probed by a variety of spectroscopic, biophysical, and chemical methods to identify the nickel ligands, deduce the coordination geometry, and characterize the nuclearity of the active site.

For native jack bean urease, electronic absorption spectroscopy revealed the presence of weak d–d absorption bands (λ_{max} at 407, 745, and 1060 nm) that were consistent with octahedral Ni(II).[8,9] The authors pointed out, however, that additional unassigned features were observed at 630, 820, and 910 nm, and that spectral comparison of a possible dinuclear center with mononuclear model compounds is not without hazard. Magnetic susceptibility measurements indicated that the urease Ni(II) ions are all high spin (μ_{eff} = 3.04(10) β/Ni) and that a majority (~75%) exhibit weak antiferromagnetic exchange coupling (J = –6 cm^{-1}), while a minor population (~25%) is magnetically isolated Ni(II).[10] This assertion was challenged, however, when data from saturation magnetization measurements on both the plant and bacterial enzymes could be fit to magneticaly isolated Ni(II) ions that were comprised of a population of high spin (S = 1) and low spin (S = 0) species, with the diamagnetic contribution increasing with increasing pH.[11] The latter results were interpreted to suggest that only a portion of the nickel is octahedral and the remainder may be a five-coordinate species with unusually low absorption intensities.

The electronic absorption spectrum is inconsistent with thiol ligation but compatible with Ni coordination by either O or N donors, a result corroborated by variable-temperature magnetic circular dichroism (MCD) spectroscopy[12] and preliminary X-ray absorption spectroscopy (XAS).[13–15] The MCD spectrum of jack bean urease exhibits two negative bands at 420 and 745 nm that increase in intensity as the temperature decreases.[12] These bands were assigned to the high-energy d–d transitions of an octahedral ligand field, and the lowest energy transition was estimated to be

* Authors to whom correspondence should be addressed.
† University of Georgia.
‡ Michigan State University.
§ Dartmouth College.
⊗ Abstract published in *Advance ACS Abstracts,* March 15, 1994.

(1) Colpas, G. J.; Maroney, M. J.; Bagyinka, C.; Kumar, M.; Willis, W. S.; Suib, S. L.; Baidya, N.; Mascharak, P. K. *Inorg. Chem.* **1991,** *30,* 920–928.
(2) Andrews, R. K.; Blakeley, R. L.; Zerner, B. In *The Bioinorganic Chemistry of Nickel*; Lancaster, J., Ed.; VCH: New York, 1988; pp 141–165.
(3) Mobley, H. L. T.; Hausinger, R. P. *Microbiol. Rev.* **1989,** *53,* 85–108.
(4) Takishima, K.; Suga, T.; Mamiya, G. *Eur. J. Biochem.* **1988,** *175,* 151–165.
(5) Mulrooney, S. B.; Hausinger, R. P. *J. Bacteriol.* **1990,** *172,* 5837–5843.
(6) Dixon, N. E.; Gazzola, C.; Blakeley, R. L.; Zerner, B. *J. Am. Chem. Soc.* **1975,** *97,* 4131–4133.
(7) Todd, M. J.; Hausinger, R. P. *J. Biol. Chem.* **1989,** *264,* 15835–15842.
(8) Dixon, N. E.; Blakeley, R. L.; Zerner, B. *Can. J. Biochem.* **1980,** *58,* 481–488.
(9) Blakeley, R. L.; Dixon, N. E.; Zerner, B. *Biochim. Biophys. Acta* **1983,** *744,* 219–229.
(10) Clark, P. A.; Wilcox, D. E. *Inorg. Chem.* **1989,** *28,* 1326–1333.
(11) Day, E. P.; Peterson, J.; Sendova, M.; Todd, M. J.; Hausinger, R. P. *Inorg. Chem.* **1993,** *32,* 634–638.
(12) Finnegan, M. G.; Kowal, A. T.; Werth, M. T.; Clark, P. A.; Wilcox, D. E.; Johnson, M. K. *J. Am. Chem. Soc.* **1991,** *113,* 4030–4032.
(13) Hasnain, S. S.; Piggott, B. *Biochem. Biophys. Res. Commun.* **1983,** *112,* 279–283.
(14) Alagna, L.; Hasnain, S. S.; Piggott, B.; Williams, D. J. *Biochem. J.* **1984,** *220,* 591–595.
(15) Clark, P. A.; Wilcox, D. E.; Scott, R. A. *Inorg. Chem.* **1990,** *29,* 579–581.

0020-1669/94/1333-1589$04.50/0

Table 1. EXAFS Data Collection and Reduction for Urease Samples

	jack bean urease native, 2-ME-treated	*K. aerogenes* urease native	*K. aerogenes* urease 2-ME-treated
SR facility	SSRL	SSRL	NSLS
beamline	2-2	7-3	X10C
monochromator crystal	Si[111]	Si[220]	Si[111]
energy resolution (eV)	~4	~1	~1
detection method	fluorescence	fluorescence	fluorescence
detector type	13-element solid-state array[a]	13-element solid-state array[b]	13-element solid-state array[c]
scan length (min)	21	21	30
scans in average	17, 13	16	8
metal concentration (mM)	~2	~2	~2
temperature (K)	11	30	48
energy standard	Ni foil (1st inflection)	Ni foil (1st inflection)	Ni foil (1st inflection)
energy calibration (eV)	8331.6	8331.6	8331.6
E_0 (eV)	8350	8350	8350
preedge background energy range (eV) (polynomial order)	8400–9040 (2)[d]	8400–9050 (2)[d]	8400–9050 (2)[d]
spline background energy range (eV) (polynomial order)	8373–8487 (2)	8378–8500 (2)	8375–8487 (2)
	8487–8716 (3)	8500–8750 (3)	8487–8716 (3)
	8716–9040 (3)	8750–9040 (3)	8716–9050 (3)

[a] Courtesy of S. P. Cramer, now at University of California, Davis. [b] Maintained by NIH Biotechnology Research Resource at SSRL. [c] Courtesy of G. N. George, now at SSRL. [d] Background was calculated by fitting this (EXAFS) region, then subtracting a constant so that the background matched the data just before the edge.

present at ~1300 nm. MCD magnetization data were not consistent with an antiferromagnetically coupled dinuclear center; rather, the behavior was described by either a ferromagnetically coupled dinuclear center or paramagnetic Ni(II) that appears to be a minor component that dominates the MCD spectrum.

The most recent XAS analysis[15] noted a generally featureless edge shape that is characteristic of pseudooctahedral geometry and identified an average Ni–O/N distance of 2.06 Å for the five or six nickel ligands. Plant and bacterial urease sequences possess several regions that are rich in histidine residues,[4,5] and chemical studies are consistent with at least partial histidyl ligation of the nickel in the native enzyme. For example, bacterial urease apoprotein was shown to be more reactive to diethyl pyrocarbonate, a histidine-selective reagent, than was holoprotein.[16] A reasonable explanation for these results is that several histidine residues in the native enzyme were inaccessible to the reagent because they serve to bind Ni. Finally, photooxidation of the jack bean enzyme in the presence of methylene blue led to the loss of activity concomitant with destruction of histidine residues.[17] This activity loss was prevented by inclusion of a specific urease inhibitor that is presumed to sterically protect the active-site residues.

A form of urease that has been intensively studied is protein in the presence of thiol-containing competitive inhibitors such as 2-mercaptoethanol (2-ME). Addition of 2-ME to jack bean or bacterial urease leads to the development of near-UV thiolate anion → Ni(II) charge transfer transitions.[7-9] The K_d values associated with thiolate-induced spectral changes match the K_i values determined kinetically for these competitive inhibitors, consistent with urea coordination to at least one nickel during catalysis. Moreover, a Ni–S scattering component with a distance of 2.29 Å was observed by XAS[15] for the thiol-bound form of the jack bean enzyme. 2-ME binding dramatically reduced the Ni(II) magnetic susceptibility of jack bean urease[10] and this was attributed to strong antiferromagnetic coupling, as ligand field[10] and XAS[15] data are not consistent with an increased amount of low-spin Ni(II). MCD spectroscopy revealed negative bands at 324, 380, 422, and 750 nm that *increased* in intensity with increasing temperature up to 150 K.[12] This anomalous temperature dependence was fit to a Boltzmann distribution of a three-level system arising from an antiferromagnetically coupled ($J = -40$ cm^{-1}) dinuclear cluster in the thiol-bound form of the enzyme. Taken together, the magnetic susceptibility, MCD, and XAS results are consistent with 2-ME bridging the two active site nickel ions; however, no Ni–Ni scattering was observed.

In this report, the metallocenter properties of plant and bacterial ureases are compared, ligands to the nickel in native and thiol-bound enzymes are determined using improved fitting procedures, and the Ni···Ni distance for the thiol-bound enzyme forms is determined.

Materials and Methods

Bacterial urease was purified from *K. aerogenes* [pKAU19][18] by previously described procedures.[7] The samples used for XAS had properties identical to those described previously.[7] These samples were apparently homogeneous with specific activities of ~2500 U/mg. Jack bean urease was isolated, purified, and assayed as described previously.[10] The properties of the native and 2-ME-treated samples analyzed in this study are identical to those described previously.[15] Metal-site concentrations in the XAS samples are given in Table 1.

X-ray absorption spectroscopic data collection was performed at both the Stanford Synchrotron Radiation Laboratory (SSRL) and the National Synchrotron Light Source (NSLS) at Brookhaven National Laboratory. Data reduction was performed using the XFPAK software package developed by one of us (R.A.S.) as described previously.[19] Details of the data collection and reduction are summarized in Table 1. The high-energy resolution used for the *K. aerogenes* urease data collection was achieved by using narrow (≤0.5 mm) vertical aperturing upstream of the monochromator. On beam line X10C at NSLS, the beam was also focused horizontally and vertically downstream of the monochromator and the vertical beam position was stabilized by feedback control of the mirror tilt angle using an in-hutch beam position monitor.

Curve-fitting analyses of the extended X-ray absorption fine structure (EXAFS) data were performed using EXCURV86 which makes use of curved-wave single- and multiple-scattering.[20] All scattering functions were calculated within EXCURV86 and verified using model compound EXAFS data. First-shell scattering functions were checked against model compound-tested FEFF v3.25[21] scattering function "templates" as described previously,[22] yielding $\Delta E_0 = 32.5$ eV, this value being fixed in all subsequent curve-fitting of urease data. (The amplitude reduction factor, AFAC, was also fixed at 0.9 for all fits.) A constrained group refinement procedure was used in fitting histidyl imidazoles. The imidazole ring was treated as a rigid group with an averaged structure taken from crystallographic data on a number of metal imidazole

(16) Lee, M. H.; Mulrooney, S. B.; Hausinger, R. P. *J. Bacteriol.* **1990**, *172*, 4427–4431.
(17) Sakaguchi, K.; Mitsui, K.; Kobashi, K.; Hase, J. *J. Biochem.* **1983**, *93*, 681–686.
(18) Mulrooney, S. B.; Pankratz, H. S.; Hausinger, R. P. *J. Gen. Microbiol.* **1989**, *135*, 1769.
(19) Scott, R. A. *Methods Enzymol.* **1985**, *117*, 414–459.
(20) Strange, R. W.; Blackburn, N. J.; Knowles, P. F.; Hasnain, S. S. *J. Am. Chem. Soc.* **1987**, *109*, 7157–7162.
(21) Rehr, J. J.; Leon, J. M. d.; Zabinsky, S. I.; Albers, R. C. *J. Am. Chem. Soc.* **1991**, *113*, 5135–5140.
(22) Scott, R. A.; Wang, S.; Eidsness, M. K.; Kriauciunas, A.; Frolik, C. A.; Chen, V. J. *Biochemistry* **1992**, *31*, 4596–4601.

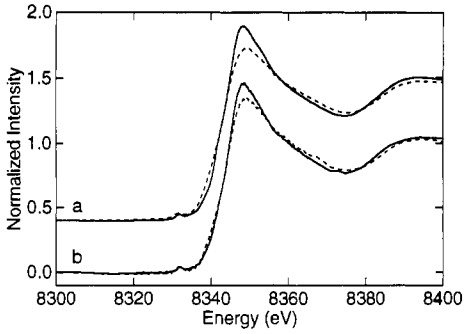

Figure 1. Nickel X-ray absorption K-edge spectra for *Klebsiella aerogenes* (a) and jack bean (b) ureases. The solid lines are the data for native samples and the dashed lines are the data for 2-ME-treated samples.

compounds. The Ni was forced to lie in the plane of the imidazole ring and only the Ni–N_1 distance and the Ni–N_1–C_2 angle were allowed to change. The position of the Ni–(N_3,C_4) multiple-scattering Fourier transform (FT) peak at ~4 Å in test simulations was compared to the experimental FT to set the Ni–N_1 distance. Tilted structures with the Ni–N_1–C_2 angle set ±5 or ±10° from that for a symmetrical imidazole were tested to match both the ~3-Å (Ni–(C_2,C_5)) and ~4-Å (Ni–(N_3,C_4)) experimental FT peaks. Once the positioning of the (average) imidazole ring was set in this way, integral coordination numbers were chosen and the Debye–Waller factors for each shell were varied to optimize the fit (with single-scattering contributions from any other required ligands included). Possible coordination numbers of histidyl imidazole ligands were selected from fits that generated physically reasonable Debye–Waller factors for these outer shells, as determined by test fits on a number of metal imidazole compounds. In a number of metal imidazole model compounds, we find that the following Debye–Waller factors are typical: M–N_1, σ_{as}^2 = 0.003–0.006 Å^2; M···(C_2,C_5), σ_{as}^2 = 0.006–0.012 Å^2; M···(N_3,C_4), σ_{as}^2 = 0.010–0.016 Å^2.

Results

The changes in the Ni X-ray absorption edge spectrum upon 2-ME addition to *K. aerogenes* urease are virtually identical to the changes reported for the jack bean enzyme.[15] Figure 1 shows that, for both enzymes, 2-ME addition results in reduced edge height and a slight shift of the lower portion of the edge to lower energy, both of these changes being consistent with increased covalency of the Ni site.[1,15] The 8332-eV 1s → 3d peak areas for the native urease spectra (normalized to unit edge height at the spline intersection with E_0) are 0.070 (jack bean) and 0.058 eV (*K. aerogenes*), larger than expected for octahedral geometry (0.006–0.040 eV) but in the range observed for five-coordinate Ni(II) sites (0.042–0.096 eV).[1] Upon 2-ME addition, these areas increase to 0.093 (jack bean) and 0.103 eV (*K. aerogenes*), at the high end of the range observed for five-coordinate Ni(II) sites and consistent with a distortion of a $Ni(N,O)_5$ site by thiolate substitution to form a $Ni(N,O)_4S$ site.[1]

For the *K. aerogenes* urease sample, first-shell curve fitting was performed as described previously for the jack bean enzyme,[15] except that FEFF scattering functions were used (see Materials and Methods). As observed for the jack bean enzyme, adequate fits to the first-shell Ni EXAFS of 2-ME-treated *K. aerogenes* urease required the presence of a shell of Ni–(S,Cl) scatterers in addition to the main Ni–(N,O) contribution, whereas the native *K. aerogenes* urease Ni EXAFS data required only a single Ni–(N,O) shell. The same result was confirmed for the jack bean urease samples in new FEFF curve fits. Both native samples are best fit with an average $Ni(N,O)_{5-6}$ coordination environment while both 2-ME-treated samples exhibit a $Ni(N,O)_{4-5}(S,Cl)_1$ environment. The Ni–ligand distances from these fits are indistinguishable from those determined by the EXCURVE fits discussed below.[23]

(23) We ascribe the slightly longer 2.29-Å Ni–S distance determined in the previous study[15] to nontransferability of the Ni–S scattering phases from the model compounds used. The current 2.23-Å Ni–S distance from FEFF curve-fitting is probably more accurate.

Table 2. Curve-Fitting Results for Ni EXAFS of Ureases[a]

sample	fit	group	shell	N_s	R_{as} (Å)	σ_{as}^2 (Å^2)	f'[b]
jack bean urease, native	A	imid	Ni–N_1	(2)[c]	2.05	0.0050	0.038
		imid	Ni–C_2		3.03	0.0070	
		imid	Ni–N_3		4.17	0.0100	
		imid	Ni–C_4		4.20	0.0100	
		imid	Ni–C_5		2.96	0.0070	
			Ni–N	(3)	2.04	0.0065	
			Ni–C	(2)	2.88	0.0085	
K. aerogenes urease, native	B	imid	Ni–N_1	(2)	2.02	0.0045	0.031
		imid	Ni–C_2		3.03	0.0070	
		imid	Ni–N_3		4.17	0.0095	
		imid	Ni–C_4		4.20	0.0095	
		imid	Ni–C_5		2.97	0.0070	
			Ni–N	(3)	2.08	0.0060	
			Ni–C	(2)	2.87	0.0045	
jack bean urease, + 2-ME	C	imid	Ni–N_1	(2)	2.05	0.0045	0.056
		imid	Ni–C_2		3.06	0.0065	
		imid	Ni–N_3		4.19	0.0100	
		imid	Ni–C_4		4.22	0.0100	
		imid	Ni–C_5		2.99	0.0070	
			Ni–N	(2)	2.03	0.0055	
			Ni–S	(1)	2.23	0.0125	
	D	imid	Ni–N_1	(2)	2.05	0.0045	0.045
		imid	Ni–C_2		3.06	0.0065	
		imid	Ni–N_3		4.19	0.0100	
		imid	Ni–C_4		4.22	0.0100	
		imid	Ni–C_5		2.99	0.0070	
			Ni–N	(2)	2.05	0.0055	
			Ni–S	(1)	2.23	0.0125	
			Ni–Ni	(1)	3.28	0.0100	
K. aerogenes urease, + 2-ME	E	imid	Ni–N_1	(2)	2.06	0.0045	0.083
		imid	Ni–C_2		3.06	0.0075	
		imid	Ni–N_3		4.19	0.0100	
		imid	Ni–C_4		4.22	0.0100	
		imid	Ni–C_5		2.99	0.0075	
			Ni–N	(2)	2.03	0.0065	
			Ni–S	(1)	2.23	0.0075	
	F	imid	Ni–N_1	(2)	2.06	0.0045	0.076
		imid	Ni–C_2		3.06	0.0075	
		imid	Ni–N_3		4.19	0.0100	
		imid	Ni–C_4		4.22	0.0100	
		imid	Ni–C_5		2.99	0.0075	
			Ni–N	(2)	2.03	0.0065	
			Ni–S	(1)	2.23	0.0075	
			Ni–Ni	(1)	3.25	0.0085	

[a] Group is the chemical unit defined for the multiple scattering calculation. N_s is the number of scatterers (or groups) per metal; R_{as} is the metal-scatterer distance; σ_{as}^2 is a mean square deviation in R_{as}. Errors in R_{as} and σ_{as}^2 are estimated to be ±0.02 Å and ±0.001 Å^2, respectively. [b] f' is a goodness-of-fit statistic normalized to the overall magnitude of the $k^3\chi(k)$ data: $f' = \{\sum[k^3(\chi_{obsd}(i) - \chi_{calc}(i))]^2/N\}^{1/2}/[(k^3\chi)_{max} - (k^3\chi)_{min}]$. [c] Numbers in parentheses were not varied during optimization.

The appearance of the outer-shell Fourier-transform (FT) peaks in the Ni EXAFS of all of the urease samples suggests the presence of histidyl imidazole ligands at the Ni(II) sites.[24] The EXCURVE curved-wave multiple-scattering formalism[20] was used to simulate this imidazole outer-shell scattering and the best average number of imidazoles per nickel was determined as discussed in Materials and Methods. For all four urease data sets, the best-fit average number of imidazoles per nickel was determined to be two (Table 2). However, the Debye–Waller σ_{as}^2 values derived for fits incorporating three imidazoles per nickel fall within (near the high end of) the expected range (see Materials and Methods) and we can therefore not rule out average imidazole coordination numbers of 3. For the native samples, as predicted by the FEFF fits, the first shell can be completely simulated by adding three more (N,O)-containing ligands at a Ni–(N,O) distance of ~2.1 Å with a reasonable Debye–Waller factor (Table 2, fits A, B). However, the ~3-Å FT peak was not simulated well with just

(24) Note that the Fourier transforms displayed in Figures 2, 3, and 4 are derived by phase correction based on Ni–N scattering. The Fourier transforms in our previous study[15] were not phase corrected and cannot be compared directly to those reported herein. We find that phase correction often results in simplification of the outer-shell region of the Fourier transform ($R' \approx 2.7$–5.0 Å), allowing EXCURVE analysis of these weaker interactions.

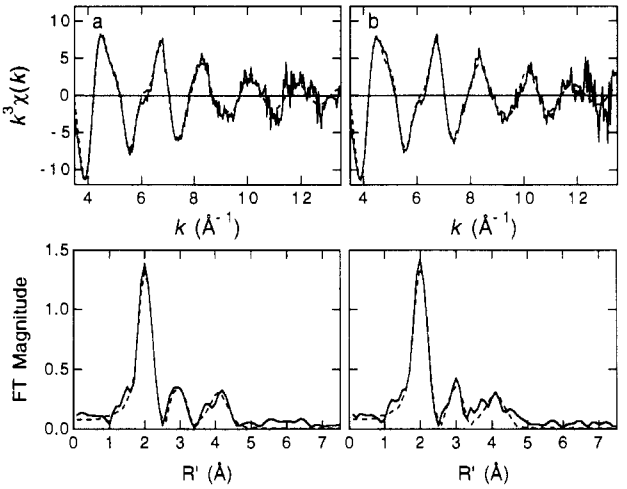

Figure 2. Nickel EXAFS (top) and Fourier transforms (bottom) for native derivatives of *K. aerogenes* (a) and jack bean (b) urease. The solid lines are the experimental data and the dashed lines the simulations using the parameters given in Table 2, fits B (a) and A (b). In Figures 2, 3, and 4, the Fourier transforms for both experimental and simulated data were performed using k^3 weighting over the k = 3.5–13.5 Å^{-1} range.

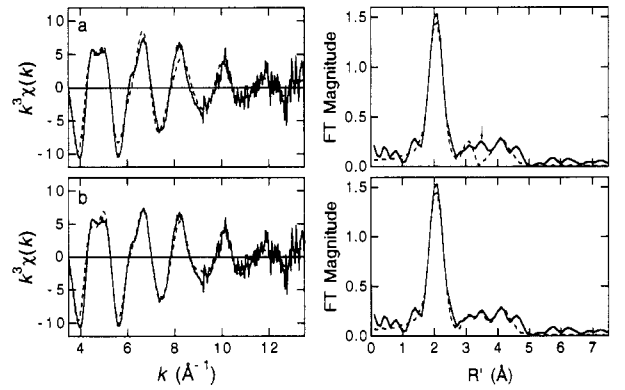

Figure 3. Nickel EXAFS (left) and Fourier transforms (right) for the 2-ME-treated derivative of *K. aerogenes* urease. The solid lines are the experimental data and curve-fitting simulations are shown as dashed lines for (a) Ni(imid)$_2$(N,O)$_2$S (fit E, Table 2) and (b) Ni(imid)$_2$-(N,O)$_2$S···Ni (fit F, Table 2). The arrow in the FT of part a indicates the peak that is assigned as the Ni···Ni scattering component.

imidazole (C_2,C_5) scattering; an extra scattering contribution from about two other carbons with Ni–C distances of 2.86 Å was required for the simulations in Table 2 (fits A, B) and Figure 2. The origin of these other carbons is unknown, but it is possible that carboxylate ligands would give rise to such a scattering component.

Initial attempts to simulate the Ni EXAFS data for the 2-ME-treated urease samples incorporated the first-shell Ni(N,O)$_4$-(S,Cl) coordination environment derived from FEFF fits, with two or three of the four first-shell (N,O)-containing ligands defined as imidazoles. Such fits (C and E, Table 2) yield reasonable first-shell distances (Ni–N_{imid} = 2.06 Å, Ni–(N,O) = 2.03 Å, Ni–(S,Cl) = 2.23 Å) and Debye–Waller factors but cannot reproduce the FT peak at $R \approx 3.6$ Å observed in both of these data sets (see arrows in the Fourier transforms of Figures 3a and 4a). Attempts to simulate this additional FT feature with Ni–X (X = C, N, O, S, Cl, Ni) resulted in improvements to the simulation only for X = Ni.[25] Incorporation of this additional Ni···Ni interaction with a Ni–Ni separation of ~3.3 Å slightly improves the goodness-of-fit parameter, f' (fits D and F, Table 2), generates an FT peak at the proper position (Figures 3b and 4b), and improves the EXAFS simulation (especially in the k = 5–10 Å^{-1} region, Figures 3b and 4b).

(25) For example, attempts to include Ni–X components in the fits for the *K. aerogenes* 2-ME-treated urease resulted in f' improvements of 3% (X = C), <1% (X = S), and 9% (X = Ni).

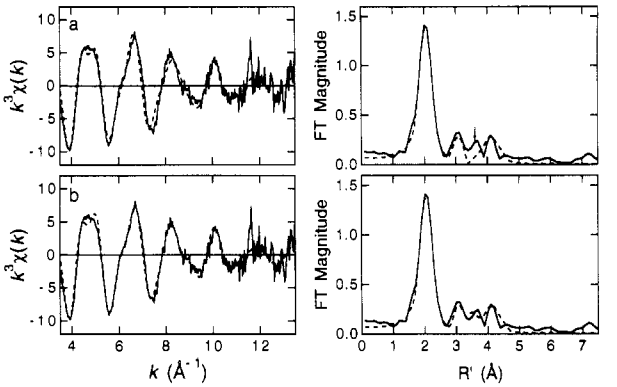

Figure 4. Nickel EXAFS (left) and Fourier transforms (right) for the 2-ME-treated derivative of jack bean urease. The solid lines are the experimental data and curve-fitting simulations are shown as dashed lines for (a) Ni(imid)$_2$(N,O)$_2$S (fit C, Table 2) and (b) Ni(imid)$_2$-(N,O)$_2$S···Ni (fit D, Table 2). The arrow in the FT of part a indicates the peak that is assigned as the Ni···Ni scattering component.

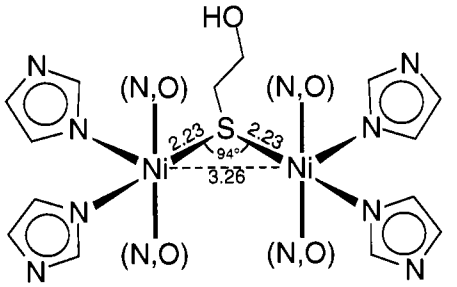

Figure 5. Proposed structure of the dinuclear Ni(II) site of 2-ME-treated urease. The arrangements and distribution of first-shell ligands around each Ni are arbitrary; there is no *a priori* reason to assume that histidyl imidazole and other (N,O)-containing ligands are distributed symmetrically. The numbers given along the Ni–S bonds and between the Ni(II) ions are distances in Å; all Ni–N(imid) and Ni–(N,O) bond lengths are ~2.05 Å (Table 2). The overall five-coordinate geometry on each Ni(II) is suggested by analysis of the Ni X-ray absorption edge spectra (Figure 1; see text for details).

Discussion

Our proposal of a ~3.3-Å Ni···Ni interaction in the 2-ME-treated urease samples is based on the ability to fit a small feature in the Fourier transform (Figures 3 and 4) with Ni···Ni scattering. As can be seen from the curve-fitting results in Table 2, the improvement in the fits upon inclusion of this Ni···Ni component is not very large (cf. fits D and F with fits C and E). Our proposal for the existence of this dinuclear site in the 2-ME-inhibited enzyme is based on a number of different pieces of evidence: (a) An extra peak appears in the FT of the 2-ME-treated samples of *both* jack bean and *K. aerogenes* ureases; (b) inclusion of Ni···Ni scattering in the EXAFS curve-fitting of the 2-ME-treated urease samples results in similar Ni···Ni distances (3.25 and 3.28 Å); (c) inclusion of Ni···Ni scattering in the EXAFS curve-fitting of the *native* urease samples yields insignificant improvement in the fits (1.7% for jack bean and 0.3% for *K. aerogenes*); (d) addition of 2-ME to urease results in strong antiferromagnetic coupling.[10,12] Taken together, these observations suggest that the effect of the inhibitor 2-ME is to establish a closer or tighter[26] association of the two Ni(II) ions in the dinuclear urease active site, resulting in a stronger magnetic exchange interaction, compared to the native site.

(26) We cannot distinguish between two possible explanations for the absence of Ni···Ni interaction in the EXAFS of the native urease samples: (a) The Ni···Ni separation is too long to be observed or (b) the Ni···Ni separation is short, but without a bridging ligand, the uncorrelated motion of the two nickels produces a large Debye–Waller factor, damping its EXAFS contribution.

The observation of an average of 1 Ni–S interaction per Ni site (Table 2, fits C–F) in the 2-ME-treated samples implies that each of the Ni(II) ions in the dinuclear site is bound by the thiolate sulfur of 2-ME. This could result from the binding of one 2-MEmolecule at each Ni(II) or from bridging of a single 2-ME molecule between the two Ni(II) of the dinuclear site. Without independent knowledge of the stoichiometry of 2-ME binding, we cannot distinguish between these two possibilities. However, bridging of the two Ni(II) by 2-ME would provide a ready explanation for the appearance of the Ni···Ni interaction in the EXAFS and for the increase in magnetic exchange interaction.[10,12] In such a hypothetical structure (Figure 5), the determined Ni···Ni distance of ~3.26 Å and Ni–S distance of 2.23 Å requires the Ni–S–Ni angle to be 94°, which is very similar to the 95–98° Ni–S–Ni angles observed in other thiolate-bridged multinuclear Ni(II) compounds.[27-31] Figure 5 also shows the rest of the Ni-(II) coordination spheres in the 2-ME-treated urease dinuclear site as suggested by the curve-fitting results in Table 2.

Acknowledgment. Dr. M. C. Brenner and Mr. Hui Zhang are thanked for assistance in the XAS data collection. Julie Breitenbach helped with some of the (earlier) *K. aerogenes* urease preparations. XAS work in the laboratory of R.A.S. is supported by the National Institutes of Health (GM 42025). Some of the XAS data were collected at the Stanford Synchrotron Radiation Laboratory (SSRL), which is operated by the Department of Energy, Division of Chemical Sciences. The SSRL Biotechnology Program is supported by the National Institutes of Health, Biomedical Resource Technology Program, Division of Research Resources. Other XAS data were collected at the National Synchrotron Light Source (NSLS), Brookhaven National Laboratory, which is supported by the U.S. Department of Energy, Division of Materials Sciences and Division of Chemical Sciences. This research was partially supported by a USDA/NRICRGO Grant (9103436) to R.P.H., by a USDA Grant (89-37120-4804) to D.E.W., and by the NSF Research Training Group Award to the Center for Metalloenzyme Studies (DIR 90-14281).

(27) Watson, A. D.; Rao, C. P.; Dorfman, J. R.; Holm, R. H. *Inorg. Chem.* **1985**, *24*, 2820–2826.
(28) Kang, B.; Weng, L.; Liu, H.; Wu, D.; Huang, L.; Lu, C.; Cai, J.; Chen, X.; Lu, J. *Inorg. Chem.* **1990**, *29*, 4873–4877.
(29) Colpas, G. J.; Kumar, M.; Day, R. O.; Maroney, M. J. *Inorg. Chem.* **1990**, *29*, 4779–4788.
(30) Lawrance, G. A.; Maeder, M.; Manning, T. M.; O'Leary, M. A.; Skelton, B. W.; White, A. H. *J. Chem. Soc., Dalton Trans.* **1990**, 2491.
(31) Capdevila, M.; Gonzalez-Duarte, P.; Foces-Foces, C.; Cano, F. H.; Martinez-Ripoll, M. *J. Chem. Soc., Dalton Trans.* **1990**, 143.